Renewable and Sustainable Energy Reviews 31 (2014) 587–599

Contents lists available at ScienceDirect

Renewable and Sustainable Energy Reviews

journal homepage: www.elsevier.com/locate/rser

A review of the mathematical models for predicting the heat and mass transfer process in the liquid desiccant dehumidifier

Yimo Luo, Hongxing Yang*, Lin Lu, Ronghui Qi

Renewable Energy Research Group (RERG), Department of Building Services Engineering, The Hong Kong Polytechnic University, Hong Kong, China

ARTICLE INFO

Article history:
Received 22 August 2013
Received in revised form
12 November 2013
Accepted 20 December 2013
Available online 21 January 2014

Keywords:
Liquid desiccant dehumidifier
Heat and mass transfer
Mathematical model

ABSTRACT

The paper aims to overview various mathematical models for modeling the simultaneous heat and mass transfer process in the liquid desiccant dehumidifier. Firstly, the dehumidification principle is introduced briefly. Then the models are interpreted in terms of two classes of dehumidifiers. For the adiabatic dehumidifier, the models are mainly classified into three types: finite difference model, effectiveness *NTU* (ε–*NTU*) model, and simplified models. For the internally cooled dehumidifier, there are also three kinds of models: models without considering liquid film thickness, models considering uniform liquid film thickness, and models considering variable liquid film thickness. This review is meaningful for comprehending the development process and research status of the models and choosing suitable models for prediction. In addition, some suggestions are proposed for the model improvement.

Contents

1. Introduction

With the acceleration of urbanization and improvement of people′ living standard, a larger proportion of building energy consumption will be needed to keep a comfortable indoor environment [1]. But it is well-known that the traditional air conditioning system is notorious as a result of heavy dependence on electric power, limited ability of humidity control, and occurrence of wet

* Corresponding author at: Office ZN 816, Department of Building Services Engineering, The Hong Kong Polytechnic University, Hong Kong, China. Tel.: +852 2766 5863.
E-mail address: hong-xing.yang@polyu.edu.hk (H. Yang).

1364-0321/$ - see front matter
http://dx.doi.org/10.1016/j.rser.2013.12.009

Nomenclature

A	specific surface area per unit volume [m^{-1}]
C_P	specific heat [$J\ kg^{-1}\ K^{-1}$]
C_{sat}	saturation specific heat [$J\ kg^{-1}\ K^{-1}$]
d_h	hydraulic diameter [m]
D_m	mass diffusion coefficient [$m^2\ s^{-1}$]
D_t	thermal diffusivity [$m^2\ s^{-1}$]
g	gravity [$m\ s^{-2}$]
G	specific mass flow rate [$kg\ m^{-2}\ s^{-1}$]
G'	mass flow rate [$kg\ s^{-1}$]
h	specific enthalpy [kJ/kg]
h_e	enthalpy of humid air in equilibrium with liquid desiccant [kJ kg]
$h_{e,eff}$	effective saturation enthalpy [kJ kg], Eq. (18)
H	height of the dehumidifier [m]
k	heat conduction coefficient [$W\ m^{-1}\ K^{-1}$]
L	length of the dehumidifier [m]
Le	Lewis number
m	water condensation rate [$g\ s^{-1}$] or per unit cross-sectional area [$g\ m^{-2}\ s^{-1}$], Eq. (23)
m^*	capacity ratio similar to the one used in sensible heat exchangers
M	molecular weight [$g\ mole^{-1}$]
NTU	number of transfer units
Nu	Nusselt number (dimensionless)
P	pressure [Pa]
P_a	partial vapor pressure in air [Pa]
P_s	partial vapor pressure over the solution [Pa]
P_t	total pressure [Pa]
$\overline{P}$	dimensionless vapor pressure difference ratio
Q	heat transferred from solution to water [$kW\ m^{-1}$]
T	temperature [K]
$\overline{T}$	dimensionless temperature difference ratio
u	velocity [$m\ s^{-1}$]
V	volume [m^3]
w	humidity ratio [$kg\ H_2O\ kg^{-1}$ dry air] or the width the dehumidifier [m]
W_e	humidity ratio of humid air in equilibrium with liquid desiccant [$kmol\ H_2O\ (kmol\ air)^{-1}$]
$W_{e,eff}$	effective humidity ratio [$kmol\ H_2O\ (kmol\ air)^{-1}$], Eq. (19)
X	desiccant concentration [kg desiccant kg^{-1}solution]
X_w	concentration of water in solution [kg water kg^{-1}solution]
X_v	concentration of water vapor in air [$kgH_2O\ kg^{-1}$]

Greek letters

α_C	heat transfer coefficient [$W\ m^{-2}\ K^{-1}$]
α'_C	heat transfer coefficient corrected for simultaneous mass and heat transfer [$W\ m^{-2}\ K^{-1}$]
α_D	mass transfer coefficient [$kg\ m^{-2}\ S^{-1}$]
α'_D	molar mass transfer coefficient [$kmol\ m^{-2}\ S^{-1}$]
ϑ	dimensionless temperatures $(T-T_r)/\overline{h}$, Eq. (33)
ρ	density [$kg\ m^{-3}$]
μ	dynamic viscosity [$kg\ m^{-1}s^{-1}$]
ν	kinetic viscosity [$m^2\ s^{-1}$]
ε	air side effectiveness
ε_{HE}	heat exchanger effectiveness
λ	latent heat of vaporization [$kJ\ kg^{-1}$]
δ	film thickness [m]
Δ	change of or difference between parameters

Subscripts

a	air
c	critical
f	cooling fluid, like water, air, refrigerant
i	inlet
int	interface
o	outlet
p	primary air
r	secondary (return air)
s	desiccant solution
v	water vapor

surface for breeding mildew and bacteria and so on [2]. Thus, to reduce the energy consumption in buildings and improve the indoor air quality, the liquid desiccant assisted air conditioning system has drawn more and more attention [3–7].

The major component of interest regarding heat and mass transfer of such a system is the dehumidifier. Compared with the experimental research, the simulation method is more time and cost saving. Also, some parameters in the dehumidifier interior can be observed by simulation while it is impossible to be achieved by experiment. Most importantly, the verified simulation models are effective tools to assess and optimize similar dehumidifiers. Therefore, a large amount of studies have been done to establish reasonable mathematical models for evaluating the liquid desiccant dehumidifiers. However, there is short of detailed and specific summary of the models until now. Thus, it is meaningful to classify and assess the models, which will provide useful suggestion for future research.

In the paper, the function principle of the liquid desiccant dehumidifier is introduced firstly. Based on whether there is heat removal, the dehumidifier is divided into two types: adiabatic and internally cooled dehumidifier. Correspondingly, the models are summarized in two respects in terms of the different structures. For each model, the assumptions, governing equations, boundary conditions and other relevant information are provided. The applied conditions, development process, and research status of the simulation models are also presented. In addition, some suggestions are put forward for the model improvement.

2. Problem description

2.1. The mechanism of heat and mass transfer in liquid desiccant dehumidifier

It is well know that in the dehumidifier, complicated heat and mass transfer occurs. The driving force for heat transfer is the temperature difference between the air and desiccant solution, and for mass transfer is the water vapor pressure difference between the air and the surface of the desiccant solution. The most classic and typical mass transfer theories include film theory, penetration theory and surface renewal theory. The theory used most for the dehumidifier is the film theory. It is Nernset [8] who proposed the film theory first in 1904. He assumed that the whole resistance of mass transfer in a given phase lied in a thin and stagnant region of that phase at the interface. This region is called film. Based on it, Whiteman [9] developed the two-film theory.

The specific transport mechanism is shown in Fig. 1. Where, P_B is the partial pressure of component B in the gas phase and X_B is the mole fraction of component B in the liquid phase.

The two film theory is very easy to understand and apply, but it has several drawbacks. Firstly, it is not reasonable to predict that the rate of mass transfer is directly proportional to the molecular diffusivity. Secondly, it is difficult to decide the thickness of the two laminar sub layers by experiment. Finally, the convective mass transfer in the thin films is neglected, so the theory is only suitable for the steady mass transfer process.

In the dehumidification process, some quantity of heat is given out as well, including the phase change heat and dilution heat. In all of the dehumidifier models, the dilution heat is neglected as it is much smaller compared with the phase change heat of water vapor [10].

2.2. Structure of the dehumidifier

As for the structure of the dehumidifier, according to whether there is heat output, the dehumidifiers can be classified into adiabatic and internally cooled dehumidifier [11]. The diagrams of two dehumidifier structures are shown in Fig. 2.

In an adiabatic dehumidifier, the air and liquid desiccant contact directly with each other. In the early stage, the research was concentrated on the structure of spray tower as a result of its simple construction and large specific surface area [12]. However, in the spray tower, the desiccant solution is generally broken into small droplets, so the problem is sometimes serious of mist generation and carryover of liquid droplets in the air stream. Then, the packed tower was used widely because it is more compact and can provide a higher residence time, lower liquid pressure loss and lessen the carryover problem. In 1980, Factor and Grossman verified the possibility of employing the packed tower as dehumidifier by theoretical analysis and experiment [13]. As for the padding materials, the random packing like ceramic [14], plastic and polypropylene pall ring are popular first [15,16]. Then some structured packing materials are employed to optimize the flow and reduce the resistance in the dehumidifier, such as the stainless steel corrugated orifice plate [17], celdek [18,19] and so on.

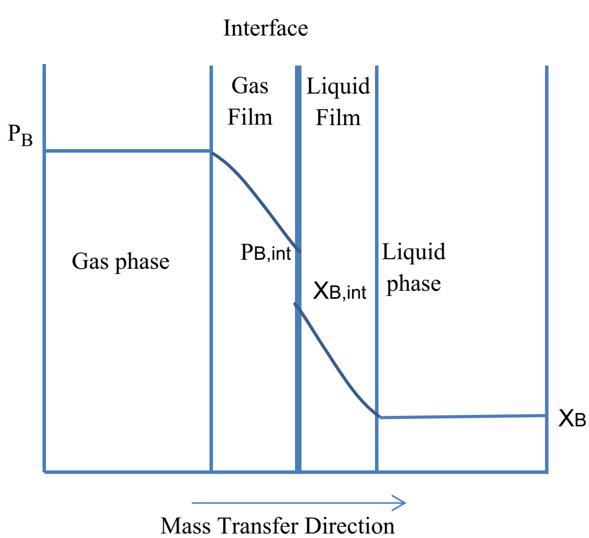

Fig. 1. Schematic diagram of two-film theory.

In the adiabatic dehumidifier, the temperature rise of the desiccant, resulted from the latent heat, worsens its dehumidification performance, thus its dehumidification efficiency is relatively lower. A solution is to increase the desiccant flow rates to achieve good dehumidification levels. However, the high desiccant flow rates and the followed higher flow rates of the regenerated desiccant solution reduce the coefficient of performance of the liquid desiccant cycle [20,21]. In addition, the desiccant particles are much easier to be entrained by the air and therefore pollute the indoor environment.

To solve the above problems, the internally cooled dehumidifier was developed. In an internally cooled dehumidifier, besides the contact between air and desiccant, some cold source which can provide cool fluid like air or water is added to take away the latent heat produced in the process of dehumidification, which can be regarded as an isothermal process in general. The internally cooled dehumidifier has been popular since the 1990s [22,23]. As the latent heat is removed from the dehumidifier, it reduces the temperature rise of the solution and air, resulting in efficiency improvement [24]. Meanwhile, it allows lower desiccant flow rates in the internally cooled dehumidifier so as to reduce the pollution problem. But the internally cooled dehumidifier has more complicated structure than the adiabatic one. For example, to increase the contact area, a fin structure is widely used in the internally cooled dehumidifier or other heat and mass transfer devices [25–29].

3. Models for adiabatic dehumidifier

There are mainly three types of mathematical models, including the finite difference model, effectiveness *NTU* (ε–*NTU*) model and the simplified solutions.

3.1. Finite difference model

In 1980, Factor et al. [13] promoted a theoretical model to predict the performance of a countercurrent packed column air–liquid contractor, based on the model for adiabatic gas absorption put forward by Treybal in 1969. In the model, the whole dehumidifier is divided into n parts, as shown in Fig. 3.

To simplify the complexity of the heat and mass transfer process, several assumptions were made: (1) the flow of air and desiccant were assumed as the slug flow, (2) the process was adiabatic, (3) the properties of the gas and liquid were assumed

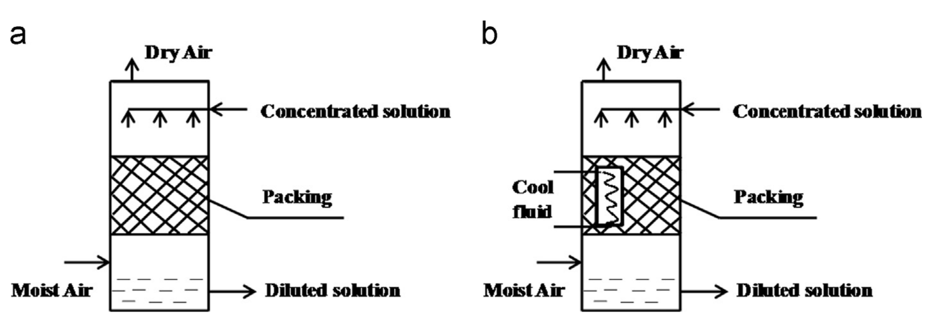

Fig. 2. The structure diagram of two dehumidifiers.

constant across the differential element, which meant the gradients only exist at the z direction, (4) both of the heat and moisture transfer areas were equal to the specific surface area of the packing, (5) it was negligible of the non-uniformity of the air and solution flows, (6) in the flow direction, no heat and moisture transfer occurred, (7) the resistance to heat transfer in the liquid phase was negligible, and (8) the interface temperature was equal to the bulk liquid temperature. Based on the above assumptions, the main governing equations were stated.

According to the mass balance in the control volume,

$$dG_s = G_a dW \tag{1}$$

According to the interface mass and sensible heat transfer rates, the air humidity change was,

$$\frac{dW}{dz} = -\frac{\alpha'_D M_v A}{G_a} \ln\left(\frac{1-P_s/P_t}{1-P_a/P_t}\right) \tag{2}$$

According to the interface sensible heat transfer from the air to solution side and the energy balance on the gas side, the air temperature change was,

$$\frac{dT_a}{dz} = -\frac{\alpha'_{C,a} A (T_a - T_s)}{G_a C_{p,a}} \tag{3}$$

$$\alpha'_{C,a} A = \frac{-G_a C_{p,v}(dW/dz)}{1-\exp[G_a C_{p,v}(dW/dz)/(\alpha_{C,a} A)]} \tag{4}$$

where $\alpha_{C,a}$ and $\alpha'_{C,a}$ are the heat transfer coefficient (sensible) of the gas side and that coefficient corrected for simultaneous mass and heat transfer by applying the Ackermann correction, which is one method to take into account the effect of mass transfer on the temperature profile with an Ackermann correction factor.

Finally, the boundary conditions were: $z=0$ $T_s=T_{s,i}$, $G_s=G_{s,i}$, $X=X_i$; $z=H$, $T_a=T_{a,i}$, $G_a=G_{a,i}$, $W=W_i$.

Since the above differential equations cannot be solved analytically, the most basic solution is a numerical integration along the height of the dehumidifier. To begin the calculation, one end of the dehumidifier must be chosen as the start point. For the countercurrent flow pattern, it needs to presume the outlet conditions for one of the fluids. Solving the above equations from the bottom to the top of the dehumidifier, with the boundary conditions, a set of calculated inlet solution parameters are obtained. By comparing the calculation results with the real values, the supposed existing

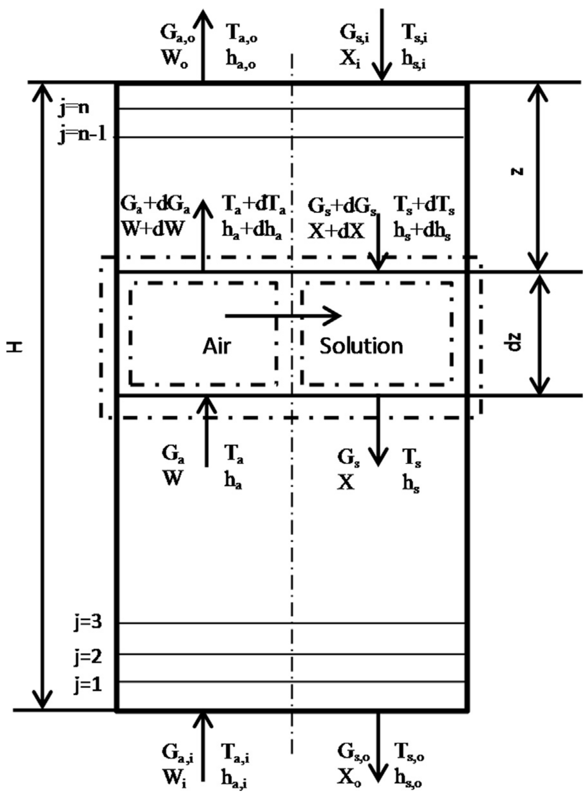

Fig. 3. Heat and moisture exchange model in the countercurrent adiabatic dehumidifier.

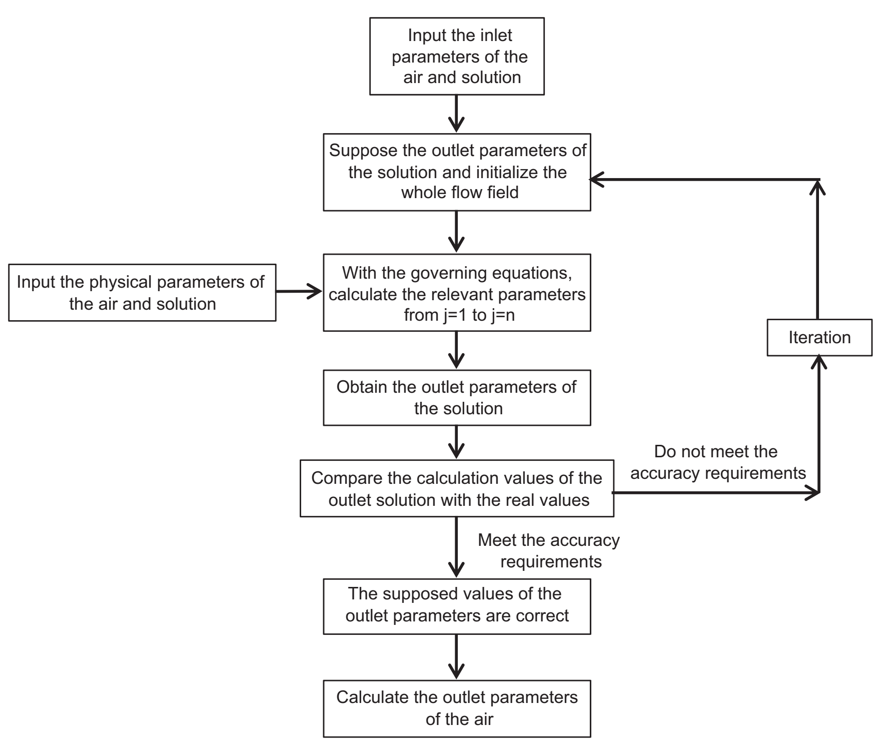

Fig. 4. Calculation flow chart of countercurrent pattern.

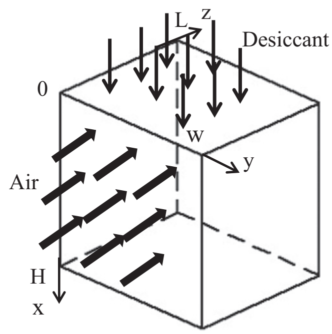

Fig. 5. Schematic of the cross flow dehumidifier/regenerator [39].

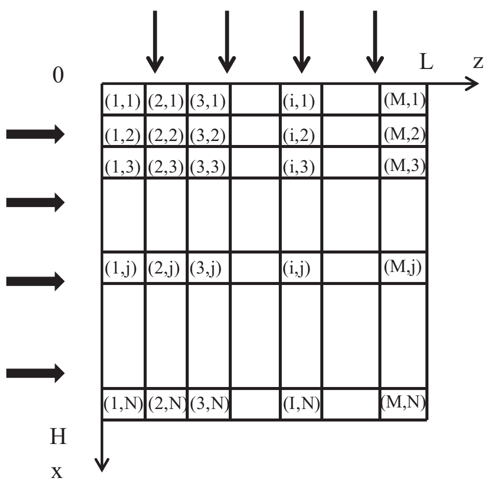

Fig. 6. A two dimensional schematic of the cross flow dehumidifier/regenerator [39].

solution variables are adjusted. The calculation will last until the final results are very close to the real values. And the general calculation flowchart for the finite difference model of the counter flow pattern can be summarized in Fig. 4.

In the later study, Gandhidasan et al. [30] utilized the similar model to study various parameters on the packing height of the packed tower. Then, Lazzarin et al. [31] gave more specific explanation of the calculation method in Appendix A of the literature. Oberg and Goswami [32] applied a finite difference model similar to Factor and Grossman′s to verify the experimental results. Taking account the insufficiently wetted packing and the different factor when transfer the *k*-type mass transfer coefficients to the *F*-type one, Fumo and Goswami [33] improved Oberg and Goswami′s mathematical model by modifying the transfer surface. In addition, a correction factor CF was introduced to modify the correlation of the wetting surface. By comparing the results of simulation and experiment, it was found that the calculation results of the adapted model agreed well with experimental results.

All of the above models introduced a coefficient $\alpha'_{C,a}$ to describe the simultaneous heat and mass transfer with the Ackermann correction. Khan and Ball [34] promoted another solution to deal with the simultaneous transfer process. Both heat and mass transfer processes were assumed to be gas controlled, so the interface temperature was the temperature of the bulk liquid and the heat transfer rate across the air film from the bulk air to the interface was equal to that entering the liquid side,

$$G_a C_{p,a} dT_a = \alpha_{C,a} A (T_s - T_a) dz \tag{5}$$

Similarly, the mass transfer across the interface was equal to the change in humidity ratio,

$$G_a dW = \alpha_{D,a} A (W_e - W) dz \tag{6}$$

Then, the humid air specific enthalpy change could be written as,

$$dh_a = C_{p,a} dT_a + dW \cdot [C_{p,v}(T_a - T_r) + \lambda] \tag{7}$$

By substituting Eqs. (6) and (7) to (5), the air enthalpy change along the flow direction was obtained. Here it is rewritten in a simpler way appeared in the later literature,

$$\frac{\partial h_a}{\partial z} = \frac{NTU \cdot Le}{H}\left[(h_e - h_a) + \lambda\left(\frac{1}{Le} - 1\right) \cdot (W_e - W)\right] \tag{8}$$

In the above equations, *Le* and *NTU* were defined as

$$Le = \frac{\alpha_C}{\alpha_D C_{p,a}} \tag{9}$$

$$NTU = \frac{\alpha_D A V}{G'_a} \tag{10}$$

In this way, the coupled heat and mass transfer were considered together. In the following research, this handling method is more popular than the Ackermann correction.

The finite difference model has been widely used for the countercurrent dehumidifier [35–38]. For cross flow configuration, Liu et al. [39] proposed a model for the heat and mass transfer process in a cross flow adiabatic liquid desiccant dehumidifier/regenerator. The physical and mathematical models are described in Figs. 5 and 6, respectively.

The governing equations of energy, water content, and solute mass balances in a differential element were,

$$\frac{G'_a}{H} \cdot \frac{\partial h_a}{\partial z} + \frac{1}{L} \cdot \frac{\partial (G'_s h_s)}{\partial x} = 0 \tag{11}$$

$$\frac{G'_a}{H} \cdot \frac{\partial W}{\partial z} + \frac{1}{L} \cdot \frac{\partial G'_s}{\partial x} = 0 \tag{12}$$

$$d(G'_s \cdot X) = 0 \tag{13}$$

The energy and mass transfer in the interface of the air and desiccant solution were expressed in Eq. (8) and the following Eq. (14),

$$\frac{\partial W}{\partial z} = \frac{NTU}{L} \cdot (W_e - W) \tag{14}$$

Like some other papers, *Le* was supposed to be one in the model. However, the value of *NTU* was correlated based on the corresponding experimental data in the paper.

Niu [40] also established a two dimensional mathematical model for the cross-flow adiabatic dehumidifier, and the mass transfer coefficient was gained from the experimental data. Woods and Kozubal [41] applied the finite difference model to study the performance of a desiccant-enhanced evaporative air conditioner and the simulation results showed good agreement with the experimental ones.

3.2. Effectiveness NTU (ε–NTU) model

Stevens et al. [42] reported an effective model for liquid-desiccant heat and mass exchanger, which was developed from a computationally simple effectiveness model for cooling towers [43]. Except for the assumptions of the finite difference model, two additional assumptions were included. One was the assumption of the linear relationship of saturation enthalpy and temperature, the other one was the neglect of the water loss term for the solution energy balance. In addition, an ‘effective’ heat and mass transfer process was assumed.

The main equations and calculation process of ε–*NTU* model were summarized as follows,

(1) Calculated the Number of Transfer Units (*NTU*) by Eq. (10).
(2) In terms of the similarity with the heat exchanger, the effectiveness of the countercurrent flow dehumidifier could be expressed as

$$\varepsilon = \frac{1-e^{-NTU(1-m^*)}}{1-m^* e^{-NTU(1-m^*)}} \tag{15}$$

where m^* was a capacitance ratio, defined analogous to the capacitance ratio used in sensible heat exchangers, and it was given in the following equations,

$$m^* = \frac{G'_a C_{sat}}{G'_{s,i} C_{p,s}} \tag{16}$$

where C_{sat} was the saturation specific heat, and $C_{sat} = (dh_e/dT_s)$.
(3) With *NTU* and ε, the air outlet enthalpy could be obtained with the following equation,

$$h_{a,o} = h_{a,i} + \varepsilon(h_e - h_{a,i}) \tag{17}$$

(4) Used an energy balance to calculate the solution outlet enthalpy.
(5) Then an 'effective' saturation enthalpy was found by

$$h_{e,eff} = h_{a,i} + \frac{h_{a,o} - h_{a,i}}{1-e^{-NTU}} \tag{18}$$

(6) Using the enthalpy and saturated conditions, the effective humidity ratio $Y_{e,eff}$ could be obtained.
(7) Then, by the following equation, the air outlet humidity ratio could be calculated,

$$W_o = W_{e,eff} + (W_i - W_{e,eff}) e^{-NTU} \tag{19}$$

(8) With the mass balance and known inlet and outlet parameters, all of the outlet parameters were acquired.

In the later study, Sadasivam and Balakrishnan [44] pointed out that the definition of *NTU* based on the gas mass velocity in Stevens's model was not appropriate when the minimum flow capacity was the liquid [45]. Thus, the gas mass velocity G'_a in Eq. (10) was changed to the minimal mass velocity of gas and liquid.

As for the ε–*NTU* model, there are much fewer literatures than the finite difference model. In the following study, Ren [46] developed the analytical expressions for the ε–*NTU* model with perturbation technique. The model accounted for the nonlinearities of air humidity ratio and enthalpy in equilibrium with solutions, the water loss of evaporation and the variation of the solution specific heat capacity.

3.3. The simplified models

It can be found that both the finite difference model and ε–*NTU* model require numerical and iterative computations. Thus, both of them are not suitable for hourly performance evaluation.

Khan and Ball [34] developed a simplified algebraic model. With the finite difference model, about 1700 groups of data were analyzed. The following functions were deduced,

$$W_o = n_0 + n_1 W_i + n_2 T_{s,i} + n_3 T_{s,i}^2 \tag{20}$$

$$W_o = m_0 + m_1 W_i + m_2 T_{a,o} + m_3 T_{a,o}^2 \tag{21}$$

The above two equations can be employed to predict the exit air temperature and humidity ratio easily. However, as they were fitted based on the data with certain operating solution concentration and solution to air mass ratio, they might not be suitable for other conditions.

Liu et al. [47] fitted some empirical correlations to estimate the performance of a cross-flow or counter-flow liquid desiccant dehumidifier. The essence of the methodology is obtaining the empirical expression of enthalpy and moisture effectiveness by experiment.

Gandhidasan [48] reported a very simple analytical solution to predicate the rate of moisture removal for the dehumidification process. Referred to previous work [49], the author promoted the dimensionless moisture and temperature difference ratios. By combining the aforementioned two definitions, the energy balance equation could be expressed as follows,

$$C_{p,a}\overline{T}(T_{a,i} - T_{s,i}) + \frac{M_v}{M_a} \cdot \frac{\lambda}{P_t} \overline{P}(P_{a,i} - P_{s,i}) = \frac{G_s}{G_a} C_{p,s}(T_{s,o} - T_{s,i}) \tag{22}$$

According to the literature [50], the relationship between the rate of moisture removal m and the partial pressure of water vapor could be deduced as

$$P_{s,i} = P_{a,i} - \frac{mP_t \; M_a}{G_a P^- \; M_v} \tag{23}$$

In addition, the desiccant outlet temperature was easily calculated, as shown in the equation,

$$T_{s,o} = \frac{T_{s,i} - \varepsilon_{HE} T_{c,i}}{(1-\varepsilon_{HE})} \tag{24}$$

Finally, substituting Eqs. (23) and (24) to (22), the moisture removal rate m was given as,

$$m = \frac{1}{\lambda}\left[\frac{G'_s C_{p,s} \varepsilon_{HE}}{(1-\varepsilon_{HE})}(T_{s,i} - T_{c,i}) - G'_a C_{p,a} \overline{T}(T_{a,i} - T_{s,i})\right] \tag{25}$$

The method was rather simple yet it involved lots of assumptions and limitations. Except some common assumptions, it also required that the desiccant inlet temperature was different from the air inlet temperature, and the desiccant temperature leaving the dehumidifier was equal to that of the desiccant entering the heat exchanger.

Chen et al. [51] constructed an analytical model on the basis of the finite difference model for countercurrent and concurrent flow pattern. The physical model is similar to that of Fig. 3. Firstly, a mathematical model was built following the model promoted by Khan and Ball [34].

Then, two parameters were introduced for derivation convenience,

$$K_a = Le \cdot C_{p,a} \cdot T_a + \lambda \cdot W \tag{26}$$

$$K_e = Le \cdot C_{p,a} \cdot T_s + \lambda \cdot W_e \tag{27}$$

By combining the mass, energy conservation equations, mass and energy transfer equations at the interface, the change of K_e along the flow direction was,

$$\frac{dK_e}{dz} = m^* \frac{NTU}{H}\left[h_{a,i} + \frac{1}{m^*}(K_e - K_{e,o}) + (Le-1)C_{p,a} \cdot T_a - K_e\right] \tag{28}$$

By integrating (28) from 0 to H or z, K_e at the outlet and along the z-axis were acquired. Based on the above results, the distribution of air enthalpy, air humidity, and temperature in a countercurrent adiabatic dehumidifier were obtained. Then, the distribution of the solution parameters can be calculated. In the paper, the analytic solution of the concurrent flow heat and mass transfer process were also given out.

Ren et al. [52] derived a new analytical solution from one-dimensional differential model. By introducing some

Table 1
Comparison of the mathematical models for adiabatic dehumidifier.

Classification	Assumption	Iteration	Accuracy	Applied situation
Finite difference model	Least	Extensive	Best	Component design and operation optimization
ε–*NTU* model	More	Less	Better	Component design and operation optimization
Simplified models	Most	No	Worst	Annual assessment

Table 2
Detail information of the mathematical models for adiabatic dehumidifier.

Classification	Model	Flow pattern	Dimensionality	Treatment of coupled, heat and mass transfer
Finite difference model	Factor et al. [13]	Counter	One-dimensional	Ackermann correction
	Oberg et al. [32]	Counter	One-dimensional	Introduction of enthalpy
	Fumo et al. [33]	Counter	One-dimensional	Ackermann correction
	Khan et al. [34]	Counter	One-dimensional	Ackermann correction
	Liu et al. [39]	Cross	Two-dimensional	Introduction of enthalpy
ε–*NTU* model	Stevens et al. [42]	Counter	One-dimensional	Introduction of enthalpy
Classification	Model	Flow pattern	Simplified method	
Simplified models	Khan et al. [34]	Counter	Correlations based on simulation results	
	Liu et al. [47]	Counter or cross	Correlations based on experimental results	
	Gandhidasan [48]	Counter	Introduction of dimensionless parameters	
	Chen et al. [51]	Counter or concurrent	Introduction of parameters similar to air enthalpy	
	Ren et al. [52]	Counter	Introduction of dimensionless parameters	
	Babakhani et al. [54]	Counter	Transfer the differential equations to nonlinear equations	
	Liu et al. [56]	Cross	Similar method of cross-flow heat exchanger	

dimensionless and dimensional groups, the conventional equations of one-dimensional model were transferred to two coupled ordinary differential equations, whose general solution are as follows,

$$\Delta W_M = C_1 e^{\lambda_1 NTU_z} + C_2 e^{\lambda_2 NTU_z} \tag{29}$$

$$\Delta \vartheta = -K_1 C_1 e^{\lambda_1 NTU_z} + K_2 C_2 e^{\lambda_2 NTU_z} \tag{30}$$

The model is just suitable for the case where the solution flow rate and concentration change slightly as it assumed that the variation of the equilibrium humidity ratio of solution depended only on the change of the solution temperature.

Babakhani and Soleymani developed analytical models for the counter flow adiabatic regenerator [53] and dehumidifier [54]. The analytical solution was deduced on the basis of the differential equations, including the mass balance, air humidity and temperature change equations listed in (1)–(3), and liquid desiccant temperature and concentration change derived from the mass and energy conservation equations. To achieve the simplification, two main assumptions were applied, including the assumptions of the dilute gas phase and constant equilibrium humidity ratio on the interface. Then the above equations could be solved and the integrated analytical solution were,

$$W = W_{int} + (W_i - W_{int})\exp(-\alpha\overline{M}NTU_z) \tag{31}$$

$$T_a = C_1 + C_2\exp(-\theta NTU_z) - \frac{\beta}{(\alpha\overline{M})^2 - \alpha\overline{M}\theta}\exp(-\alpha\overline{M}NTU_z) \tag{32}$$

$$T_s = \frac{1}{R_c Le}\left[-C_2\theta\exp(-\theta NTU_z) + \frac{\alpha\overline{M}\beta}{(\alpha\overline{M})^2 - \alpha\overline{M}\theta}\exp(-\alpha\overline{M}NTU_z)\right] + T_a \tag{33}$$

$$InX = -R_m(W_i - W_{int})\exp(-\alpha\overline{M}NTU_z) + C_3 \tag{34}$$

$$G_s = G_a(W_i - W_{int})\exp(-\alpha\overline{M}NTU_z) + C_4 \tag{35}$$

With the above solutions, the profiles of the outlet solution and air parameters were available.

Based on the above model, Babakhani [55] also developed another analytical model which was well suited to the high desiccant flow rate conditions.

Liu et al. [56] developed an analytical solution for a similar cross-flow packed bed liquid desiccant air dehumidifier, whose numerical model had been reported in literature [39]. In the present work, it was regarded that the desiccant mass flow rate and concentration kept constant in the whole process. Thus the Eqs. (12)–(14) were got rid of, and only Eqs. (8) and (11) were left for calculation, which were rewritten as

$$m^* \cdot \frac{\partial h_a}{\partial z} + \frac{H}{L} \cdot \frac{\partial h_e}{\partial x} = 0 \tag{36}$$

$$\frac{\partial h_a}{\partial z} = -\frac{NTU}{L} \cdot (h_a - h_e) \tag{37}$$

It was found the above control equations had high similarity with those of the cross-flow heat exchanger. Thus the methods in literature [57,58] were referred to. As the solution expressions were a litter complicated, here they will not be presented.

Recently, Wang et al. [59] developed a simplified yet accurate model for real-time performance optimization. Levenberg–Marquardt method was used to identify the parameters. The proposed model is suggested to be employed in real-time performance monitoring, control and optimization. Park and Jeong [60] also developed a simplified second-order equation model as a function of operation parameters to study their impact on the dehumidification effectiveness.

3.4. Summary

To sum up, there are three models to simulate the adiabatic dehumidifiers. The general comparison of them is presented in Table 1. As a matter of convenience, the information of some representative models is summarized in detail in Table 2.

The finite difference model is used most frequently for its accuracy. However, it involves complicated iterative process, so it is only suitable for the component design and operation optimization. The common assumptions have been stated in Factor's model. However, some other simplifications or improvements are made to satisfy the real conditions. It can also be observed that counter flow configuration is the most commonly used flow pattern, and it can be described by the one-dimensional model. For the dehumidifier with cross flow configuration, the problem is generally solved by the two-dimensional model.

For the *ε–NTU* model, two additional assumptions are included as mentioned above. Thus, the model is less accurate than the finite difference model. However, compared with the finite difference model, the calculations are dramatically less extensive. Thus, the *ε–NTU* model has great potential for saving time. But with the development of the computer technology, the calculated amount of the finite difference model can be accepted due to its accuracy. Therefore, much fewer researches have been done on the *ε–NTU* model in the later studies.

From Table 2, it is concluded that different dimensionless parameters have been introduced in the deviation processes of the simplified models. Meanwhile, the additive assumptions are needed for simplification. Therefore, they are only applicable for certain operation conditions, and different models can be chosen to be suited to the real situation. The biggest advantage of these models is that the iteration is avoided. As a result of their high efficiency, they are often used to predict the annual energy consumption of an air-conditioning system.

4. Models for internally cooled dehumidifier

In the internally cooled dehumidifier, some cooling fluid is introduced to remove the heat produced by the vapor condensation, as shown in Fig. 7 [61]. Most of the models for the internally cooled dehumidifier are developed upon the finite difference methods used for the adiabatic dehumidifier. The difference is the additional consider of the heat transfer brought by the cooling media. In addition, because of the relatively low solution flow rate in the internally cooled dehumidifier, it is easier for the solution to form a thin film on the surface of the padding wall or plate. Briefly, there are also three types of models for the internally cooled dehumidifier.

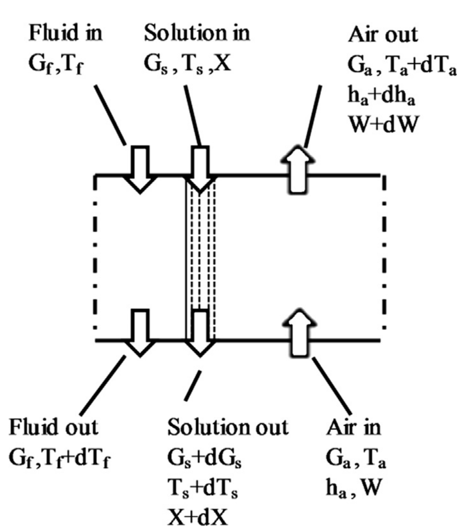

Fig. 7. Heat and moisture exchange model in the internally cooled dehumidifier [61].

4.1. Models without considering liquid film thickness

The first type ignores the liquid film thickness. Khan and Martinez [62] developed a mathematical model to predict the performance of a liquid desiccant absorber integrating indirect evaporative cooling to achieve an almost isothermal operation. The processed air and the solution flowed in countercurrent direction while the solution and water flowed in parallel direction.

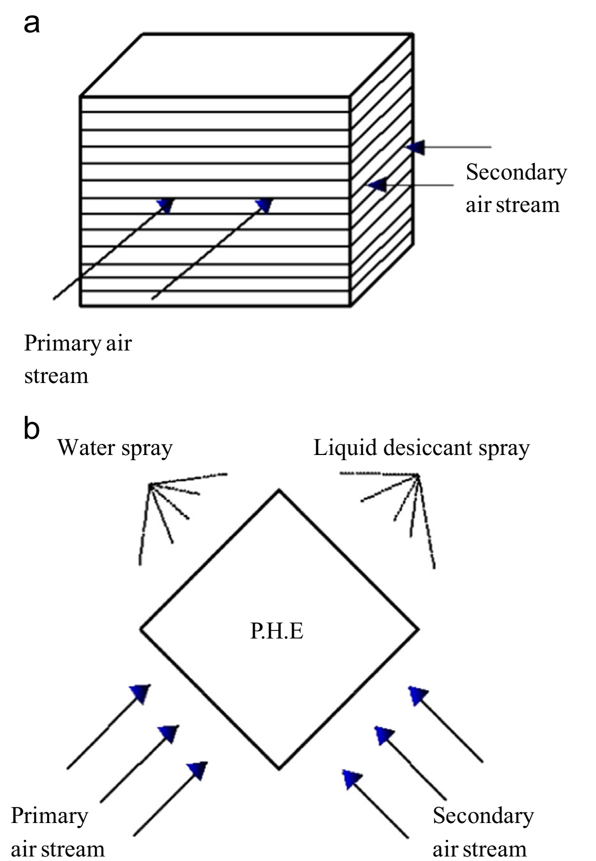

Fig. 8. Schematic diagram of the cross-flow type plate heat exchanger [61].

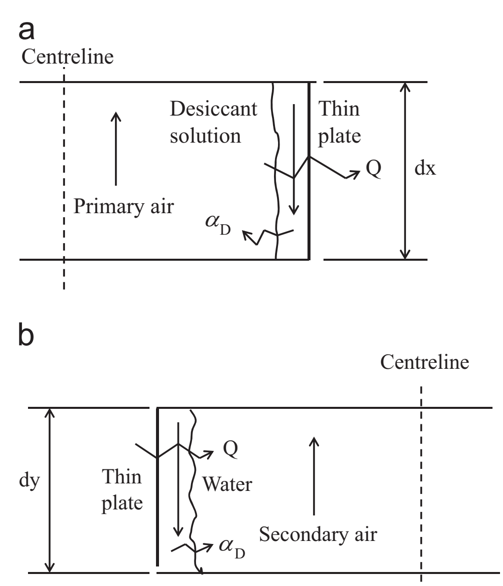

Fig. 9. Schematic diagram of the control volumes considered: (a) primary air-solution; (b) secondary air–water [63].

Saman and Alizadeh [63] also established a similar model for a cross-flow type plate heat exchanger (PHE) serving as internally cooled dehumidifier. The schematic diagrams of the PHE are presented in Figs. 8 and 9. It is obviously that it has the same principle with that in literature [62]. The only difference lies in the configuration difference. Here, Saman's model will be explained in detail as it is more representative. In the paper, the PHE was divided into a certain number of control volumes in two orthogonal directions. Several assumptions were set, including no heat transfer with the environment, negligible temperature gradient between the solution film and water film, and fully cover of solution and water on the plate.

Thus, the change of the enthalpy and humidity ratio of the primary air were,

$$\frac{dh_{a,p}}{dx}=\frac{NTU_s\cdot Le_s}{H}\left[(h_{e,s}-h_{a,p})+\lambda\left(\frac{1}{Le_s}-1\right)\cdot(W_{e,s}-W_p)\right] \tag{38}$$

$$\frac{dW_p}{dx}=\frac{NTU_s}{H}\cdot(W_{e,s}-W_p) \tag{39}$$

Also, the mass and energy conservation equations in the control volume were given as

$$G'_{a,p}\cdot\frac{dW_p}{dx}-\frac{dG'_s}{dx}=0 \tag{40}$$

$$G'_{a,p}\cdot\frac{dh_{a,p}}{dx}-\frac{d(G'_s h_s)}{dx}+Q=0 \tag{41}$$

Similarly, the change of the enthalpy and humidity ratio of the secondary air, and mass and energy conservation equations were expressed as follows

$$\frac{dh_{a,r}}{dy}=\frac{NTU_f\cdot Le_f}{H}\left[(h_{e,f}-h_{a,r})+\lambda\left(\frac{1}{Le_f}-1\right)\cdot(W_{e,f}-W_r)\right] \tag{42}$$

$$\frac{dW_r}{dx}=\frac{NTU_f}{H}\cdot(W_{e,f}-W_r) \tag{43}$$

$$G'_{a,r}\cdot\frac{dW}{dy}-\frac{dG'_f}{dy}=0 \tag{44}$$

$$G'_{a,r}\cdot\frac{dh_{a,r}}{dy}-\frac{d(G'_f h_f)}{dy}-Q=0 \tag{45}$$

On the basis of the above governing equations, the discretization equations were derived for each control volume. The calculation method was similar to the flow chart of the finite difference model presented in Fig. 4, while it was more complicated as a result of another iteration started by the advance assumption of the cooling water temperature. In the paper, it is noted that the film thickness was mentioned, but the simulation did not take it into consideration.

Liu et al. [21] compared the performances of internally cooled dehumidifiers with various flow patterns. A representative heat and mass transfer model was selected for detail description, as shown in Fig. 10. Referred to literature [34], the heat and humidity changes of the air were almost the same with the Eqs. (6) and (8).

The energy conservation equation was expressed as

$$G'_a\cdot\frac{\partial h_a}{\partial x}=\frac{\partial(G'_s h_s)}{\partial x}+C_{p,f}G_f'\frac{L\,\partial T_f}{H\,\partial y} \tag{46}$$

As the mass conservation equation has been explained before, here it will not be presented for limited space. And the heat transfer between the desiccant solution and the cooling water was,

$$\frac{\partial T_f}{\partial y}=\frac{NTU_f}{L}\cdot(T_s-T_f) \tag{47}$$

Combined the above equations with the inlet conditions, the distribution of the parameters of the air, desiccant solution, and the cooling water could be obtained. The model was applied for

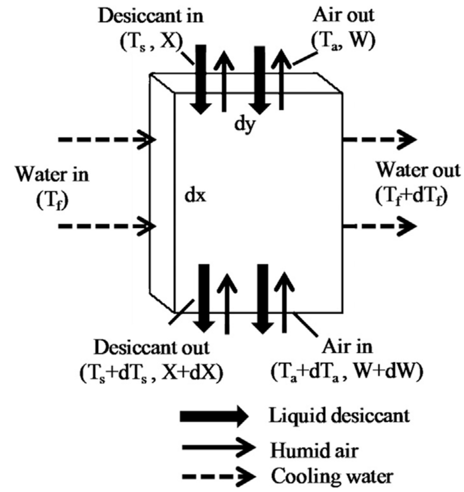

Fig. 10. Schematic diagram of the control volume for a counter-flow internally cooled dehumidifier [21].

analyzing the role of flow patterns in depth, which was seldom reported in previous literatures. In the later study, Zhang et al. [64] employed the above model to predict the performance of an internally-cooled dehumidifier.

Yin et al. [25] built a uniform mathematical model for an internally cooled/heated dehumidifier/regenerator which was made up of a plate heat exchanger. It is important to point out that the author took the non-wetted area into consideration by introducing the wetness coefficient. Meanwhile, in a control volume, the transfer process in the channel width was considered to be symmetrical. In addition, to improve the accuracy of the model, the author also applied the correlation of the mass transfer coefficient fitted out by experiment [24].

Based on the one-dimensional differential equations for the heat and mass transfer processes with parallel or counterflow configurations, Ren et al. [61] developed an analytical model for internally cooled or heated liquid desiccant-air contact units. To increase the accuracy, the model took the effects of solution film heat and mass transfer resistances, the variations of solution mass flow rate, non-unity values of Lewis factor and incomplete surface wetting conditions into consideration.

Recently, Qi et al. [65,66] developed a simplified model to predict the performance of the internally cooled/heated liquid desiccant dehumidification system. Compared to previous study, all of the outlet parameters could be obtained by the correlations quickly and accurately. Thus, it is very useful for researching the dynamic operation performance of the internally cooled/heated liquid desiccant dehumidification system.

Khan and Sulsona [28] developed a two-dimensional and steady-state model for a vapour compression/liquid desiccant hybrid cooling and dehumidification absorber made up of the tube-fin exchanger. To simplify the model, several assumptions were made reasonably. The most critical one was to consider the air and refrigerant flow in countercurrent due to the large size in the air flow direction. In this way, the complicated problem was simplified to a two-dimensional one. The governing equations are very similar to those of literature [21] except for the mass conservation equation. There were three iterations: one for the real refrigerant exit enthalpy, one for the correct local coil surface temperature and the final one for the actual solution temperature.

4.2. Models considering uniform liquid film thickness

In the second model, the film is considered as a uniformly distributed desiccant film.

Park et al. [26] developed a three dimensional numerical model for simulating the coupled heat and mass transfer in a cross-flow internally cooled/heated dehumidifier/regenerator. The schematic diagram was presented in Fig. 11. Some assumptions were used before listing out the governing equations: the flow was considered as laminar and steady; the physical properties for both solution and air were constant; species thermo-diffusion and diffusion-thermo effects were negligible and thermodynamic equilibrium existed at the solution–air interface. Because of the relatively small absorption, the TEG solution film thickness was simplified as constant and the film mean velocity was also unchanged. Also, the velocity gradient in the liquid solution film at the interface was regarded as zero and the flow of the liquid solution and air was supposed to be fully developed at the start place, as presented in Fig. 11.

With the assumptions, the governing equations for the liquid solution flow were,

$$0=\mu_s\frac{\partial^2 u_s}{\partial y_1^2}+\rho_s g \tag{48}$$

$$u_s\frac{\partial T_s}{\partial x}=D_{t,s}\frac{\partial^2 T_s}{\partial y_1^2} \tag{49}$$

$$u_s\frac{\partial X_w}{\partial x}=D_{m,s}\frac{\partial^2 X_w}{\partial y_1^2} \tag{50}$$

For the air flow, the governing equations were as follows,

$$0=-\frac{dP}{dz}+\mu_a\frac{\partial^2 u_a}{\partial y_2^2} \tag{51}$$

$$u_a\frac{\partial T_a}{\partial z}=D_{t,a}\frac{\partial^2 T_a}{\partial y_2^2} \tag{52}$$

$$u_a\frac{\partial X_v}{\partial z}=D_{m,a}\frac{\partial^2 X_v}{\partial y_2^2} \tag{53}$$

At the interface, the mass and energy balances also existed,

$$\rho_s D_{m,s}\frac{\partial X_w}{\partial y_1}=-\rho_a D_{m,a}\frac{\partial X_v}{\partial y_2} \tag{54}$$

$$-k_s\frac{\partial T_s}{\partial y_1}=k_a\frac{\partial T_a}{\partial y_2}+\rho_a D_{m,a}\frac{\partial X_v}{\partial y_2}\lambda \tag{55}$$

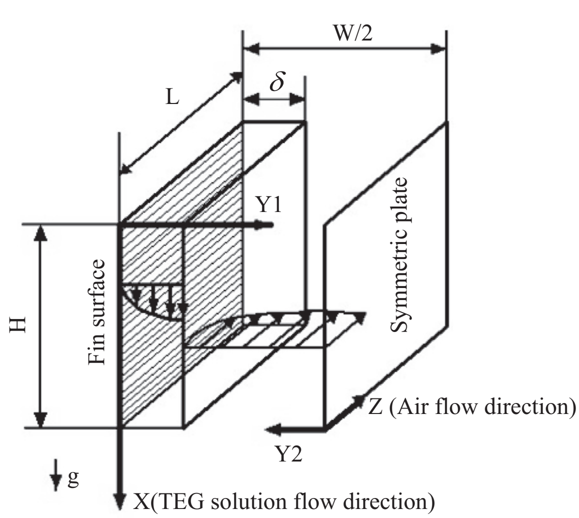

Fig. 11. Schematic diagram of control volume for a three-dimensional model [26].

The above equations can be discretized along the three different directions. Being combined with the boundary and interfacial conditions, the equations could be solved.

Ali et al. [67–69] had used the same mathematical model to study the effect of the flow configuration, the inclination angle, the Reynolds numbers, various inlet parameters, cu-ultrafine particles volume fraction, and thermal dispersion on the performance of the dehumidifier/regenerator.

Mesquita et al. [70] compared three different numerical models for parallel plate internally cooled liquid desiccant dehumidifier. The second one introduced a constant film thickness. It was assumed that the wall was isothermal so that the water flow could be neglected. On the basis of some other assumptions, the dehumidification process could be described by a two dimensional model, as shown in Fig. 12. Being different from the first model which does not consider the film thickness, this model took the momentum equations into consideration. Firstly, the velocity profiles of the air and liquid desiccant were obtained with the momentum equations, presented as follows,

$$\delta=\left(\frac{3G_s'\nu_s}{\rho_s g}\right)^{1/3} \tag{56}$$

$$u_s=\frac{3G_s'}{2\rho_s}\left(\frac{2y}{\delta^2}-\frac{y^2}{\delta^3}\right) \tag{57}$$

$$u_a=u_s+\frac{dP}{dx}\frac{1}{\mu_a}\left[\frac{1}{2}(y^2-\delta^2)+\left(\frac{W}{2}-y\right)\right] \tag{58}$$

$$\frac{dP}{dx}=3\mu_a\left[\frac{u_s}{(\delta-W/2)^2}+\frac{G_a'}{2\rho_a(\delta-W/2)^3}\right] \tag{59}$$

The energy and species equations of the liquid phase, gas phase, and the energy and species balances equations at the interface are almost the same with those presented in literature [26]. Then with the velocity values and boundary conditions, all the above equations could be solved numerically and simultaneously with the software package Microsoft EXCEL.

Recently, Dai and Zhang [71] employed the uniform liquid film thickness to evaluate the performance of a cross flow liquid desiccant air dehumidifier packed with honeycomb papers. The objective of the paper is to analyze the Nusselt and Sherwood numbers in the channels with honeycomb papers as the packing materials.

4.3. Models considering variable liquid film thickness

The final model introduces a variable film thickness. Except the constant thickness model, Mesquita et al. [70] also established

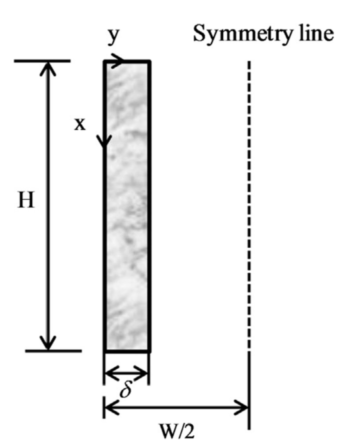

Fig. 12. Schematic diagram of control volume for a two-dimensional model [70].

Table 3
Detail information of the mathematical models for internally cooled dehumidifier.

Classification	Model	Flow pattern (air/desiccant)	Flow pattern (desiccant/cooling fluid)	Cooling fluid
Regardless of film thickness	Khan et al. [62]	Counter	Counter	Water and air
	Saman et al. [63]	Counter	Cross	Water and air
	Liu et al. [21]	Six different configurations		Water
	Yin et al. [25]	Cocurrent	Cocurrent	Water
	Khan et al. [28]	Cross	Cross	Ammonia
	Ren et al. [61]	Four possible flow arrangements		–
Uniform film thickness	Park et al. [26]	Cross	Cross	R22
	Ali et al. [67–69]	Cocurrent/counter/cross	–	–
	Mesquita et al. [70]	Counter	Counter	Water
	Dai et al. [71]	Cross	–	–
Variable film thickness	Mesquita et al. [70]	Counter	Counter	Water
	Hueffed et al. [72]	Cross	–	–
	Peng et al. [73]	Counter	–	–
	Diaz [74]	Cocurrent	–	–

another variable thickness model for internally cooled liquid-desiccant dehumidifiers. In the model, the film thickness in Eq. (56) varied, thus for every step of calculation, the film thickness was recalculated, so was the liquid velocity profile in Eq. (57). However, to reduce the computational time, the change in the airflow velocity profile was neglected as a result of the small film thickness changes. Compared the results of variable thickness model with the constant thickness model, it was found that the two models converged to the same results at higher desiccant flow rates. However, the constant thickness model underestimated the dehumidification for low desiccant flow rates.

Hueffed et al. [72] presented a simplified model for a parallel-plate dehumidifier, with both adiabatic and isothermal absorption. The model used a control volume approach and accounted for the film thickness variation by imposing its effect on the heat and mass transfer coefficients. The specific equations of the heat transfer coefficient in terms of the film thickness were listed as

$$\alpha_C = \frac{Nuk_a}{d_h} \tag{60}$$

$$d_h = 2(W - 2\delta) \tag{61}$$

Then the mass transfer coefficient was obtained from the Chilton–Coulburn analogy as

$$\alpha_D = \frac{\alpha_C}{C_{p,a}}\left(\frac{D_t}{D_{m,a}}\right)^{-2/3} \tag{62}$$

In each control volume, various parameters, including the film thickness δ, hydraulic diameter d_h, heat transfer coefficient α_C, and mass transfer coefficient α_D were calculated on the basis of the inlet conditions. In this way, the impact of the film thickness variation on the heat and mass transfer process were introduced into the model.

Recently, Peng and Pan [73] investigated the transient performance of the liquid desiccant dehumidifier with a one-dimensional non-equilibrium heat and mass transfer model. Unlike the previous study, the local volume average equations of heat and mass transfer were developed in the work, which were solved by *Tri*Diagonal-Matrix Algorithm (TDMA).

In the later year, Diaz [74] also developed a transient two dimensional model for a parallel-flow liquid-desiccant dehumidifier. The geometrical model was almost the same with that of Mesquita et al. [70]. The difference of the governing equations lies in that the present model took the time item into consideration. Some non-dimensional parameters were used to simplify the calculation process. With the model, the variations of some critical variables over time were illustrated and the effects of oscillatory behavior were analyzed in depth.

4.4. Summary

The detail information of the mathematical models for the internally cooled dehumidifier is listed out in Table 3.

The models for internally cooled dehumidifier without considering the film thickness are very similar to those used in the adiabatic dehumidifier. However, the former ones are more complicated due to the involvement of the cooling fluid. These models ignore the effect of the velocity field. Thus, the results of these models have certain discrepancy with the reality, as velocity, mass and energy have strong coupling relationship.

In the models considering uniform film thickness, the film thickness and velocity are usually calculated at the beginning and then keep constant through the whole calculation. The simulation results justified that the constant thickness models under-predicted the dehumidification, especially for low desiccant mass flow rate.

For the models considering variable film thickness, all of the velocity, mass and energy equations are solved together. In the process of each iteration, the film thickness and velocity change, so the influence of the flow on the heat and mass transfer can be demonstrated. Thus, the model is most accurate.

5. Conclusion

Various mathematical models have been proposed to assess the performance of the liquid desiccant dehumidifiers. For the adiabatic dehumidifier, there are mainly three kinds of models: finite difference model, ε–*NTU* model, and simplified models. The finite difference model is used most widely for its accuracy. However, it involves complicated iterative process which increases the computer time, so it is only suitable for the design of the component and optimization of the operating conditions. Like the finite difference model, the ε–*NTU* model also requires iteration, but it is more effective and less accurate correspondingly. The simplified models require more assumptions, so they are only suitable in certain operation conditions. But due to their high efficiency, they are often used to predict the annual performance of the system.

For the internally cooled dehumidifier, there are also three kinds of models: models without considering liquid film thickness, models considering uniform liquid film thickness, and models considering variable liquid film thickness. The first model ignores the effect of the velocity field totally. Thus, the calculation results

have certain discrepancy with the reality. The second one consider the effect of the velocity field, but the assumption of the steady state and fully developed field cannot describe the real condition, especially for low desiccant mass flow rate. The final model is most accurate as it comprehensively regards the influence of the changed velocity field, but the calculation becomes relatively complicated.

Though a large amount of researches have been conducted on modeling and analyzing the liquid desiccant dehumidifier, further efforts are still needed:

(1) The vast majority of the previous models assume the heat and mass transfer process to be steady state and more transient models to study the dynamic performance are needed.
(2) More three-dimensional models close to the reality are needed.
(3) Most of the models focus on the outlet parameters and more research are required to study the heat and mass transfer process in the dehumidifier interior.
(4) It needs to take into consideration the effect of variable physical properties which are taken as constant in almost all existing models.

Acknowledgments

The work described in this paper was supported by the Hong Kong PhD Fellowship Scheme.

References

[1] Jiang Y. Current building energy consumption in China and effective energy efficiency measures. Heat Vent Air Cond 2005;35:30–40 (in Chinese).
[2] Ge GM, Xiao F, Niu XF. Control strategies for a liquid desiccant air-conditioning system. Energy Build 2011;43(6):1499–507.
[3] Liu XH, Li Z, Lin BR. Annual performance of liquid desiccant based independent humidity control HVAC system. Appl Ther Eng 2006;26(11–12):1198–207.
[4] Potnis SV, Lenz TG. Dimensionless mass-transfer correlations for packed-bed liquid desiccant contactors. Ind Eng Chem Res 1996;35(11):4185–93.
[5] Oberg V, Goswami DY. Advances in solar energy: an annual review of research and development. Am Sol Energy Soc Inc. 1998;12:431–70.
[6] Xie XY, Jiang Y, Tang YD, Yi XQ, Liu SQ. Simulation and experimental analysis of a fresh air-handling unit with liquid desiccant sensible and latent heat recovery. Build Simulation 2008;1:53–63.
[7] Jiang Y, Li Z. Dehumidification air conditioning method and systems; 2002. (in Chinese)
[8] Nernst W. Theory of reaction velocity in heterogenous systems. Z Phys Chem 1904;47:52–5.
[9] Whitman W. The two-film theory of gas absorption. Chem Metall Eng 1923;29(4):146–8.
[10] Lowenstein AI, Gabruk RS. The effect of absorber design on the performance of a liquid-desiccant air conditioner. ASHRAE Trans 1992:712–70 (Symposia).
[11] Keslling W, Laevemann E, Kapfhammer C. Energy storage for desiccant cooling systems component development. Sol Energy 1998;64:209–21.
[12] Zhao Y, Shi MH. Comparison of dehumidifier in solar liquid desiccant air-conditioner system. Acta Energiae Sol Sin 2002;23(1):1–4 (in Chinese).
[13] Factor HM, Grossman GA. packed bed dehumidifier/regenerator for solar air conditioning with liquid desiccants. Sol Energy 1980;24(6):541–50.
[14] Sadasivam M, Balakrishnan AR. Experimental investigation on the thermal effects in packed-bed liquid desiccant dehumidifiers. Ind Eng Chem Res 1994;33(6):1636–40.
[15] Chung TW, Wu H. Mass transfer correlation for dehumidification of air in a packed absorber with an inverse u-shaped tunnel. Sep Sci Technol 2000;35(10):1503–15.
[16] Longo GA, Gasparella A. Experimental analysis on chemical dehumidification of air by liquid desiccant and desiccant regeneration in a packed tower. J Sol Energy Eng 2004;126(1):587–91.
[17] Yang Y. Experimental study on the characteristic of liquid dehumidification system [Master thesis]. Tianjing University; 1999. (in Chinese).
[18] Chung TW, Ghosh TK, Hines AL, Novosel D. Dehumidification of moist air with simultaneous removal of selected indoor pollutants by triethylene glycol solutions in a packed-bed absorber. Sep Sci Technol 1995;30(7):1807–32.
[19] Elsarrag E, Magzoub EEM, Jain S. Mass-transfer correlations for dehumidification of air by triethylene glycol in a structured packed column. Ind Eng Chem Res 2004;43:7676–81.
[20] Khan AY. Cooling and dehumidification performance analysis of internally-cooled liquid desiccant absorbers. Appl Ther Eng 1998;18(5):265–81.
[21] Liu XH, Chang XM, Xia JJ, Jiang Y. Performance analysis on the internally cooled dehumidifier using liquid desiccant. Build Environ 2009;44:299–308.
[22] Bansal P, Jain S, Moon C. Performance comparison of an adiabatic and an internally cooled structured packed-bed dehumidifier. Appl Ther Eng 2011;31:14–9.
[23] Chung TW, Wu H. Comparison between spray towers with and without fin coils for air dehumidification using triethylene glycol solutions and development of the mass-transfer correlations. Ind Eng Chem Res 2000;39:2076–84.
[24] Yin YG, Zhang XS, Wang G, Luo L. Experimental study on a new internally cooled/heated dehumidifier/regenerator of liquid desiccant systems. Int J Refrig 2008;31:857–66.
[25] Yin YG, Zhang XS, Peng DG, Li XW. Model validation and case study on internally cooled/heated dehumidifier/regenerator of liquid desiccant systems. Int J Ther Sci 2009;48:1664–71.
[26] Park MS, Howell JR, Vliet GC, Peterson J. Numerical and experimental results for coupled heat and mass transfer between a desiccant film and air in cross-flow. Int J Heat Mass Transfer 1994;37(Suppl):395–402.
[27] Qin F, Shao SQ, Luo YM, Tian CQ, Zhang GY. Investigation of performance of fin-tube internally heated regenerator in liquid desiccant air conditioning system. In: Proceedings of the international conference on applied energy, Suzhou, China; 2012.
[28] Khan AY, Sulsona FL. Modelling and parametric analysis of heat and mass transfer performance of refrigerant cooling liquid desiccant absorbers. Int J Energy Res 1998;22(9):831–2.
[29] Jain S, Bansal PK. Performance analysis of liquid desiccant dehumidification systems. Int J Refrig 2007;30:861–72.
[30] Gandhidasan P, Ullah MR, Kettleborough CF. Analysis of heat and mass transfer between a desiccant-air system in a packed tower. J Sol Energy Eng 1987;109:89–93.
[31] Lazzarin RM, Gasparella A, Longo GA. Chemical dehumidification by liquid desiccants: theory and experiment. Int J Refrig 1999;22:334–47.
[32] Oberg V, Goswami DY. Experimental study of the heat and mass transfer in a packed bed liquid desiccant air dehumidifier. J Sol Energy Eng 1998;120(4):289–97.
[33] Fumo N, Goswami DY. Study of an aqueous lithium chloride desiccant system: air dehumidification and desiccant regeneration. Sol energy 2002;62(4):351–61.
[34] Khan AY, Ball HD. Development of a generalized model for performance evaluation of packed-type liquid sorbent dehumidifiers and regenerators. ASHRAE Trans 1992;98:525–33.
[35] Gandhidasan P, Kettleborough CF, Ullah MR. Calculation of heat and mass transfer coefficients in a packed tower operating with a desiccant-air contact system. J Sol Energy Eng 1986;108:123–8.
[36] Elsayed MM, Gari HN, Radhwan AM. Effectiveness of heat and mass transfer in packed beds of liquid desiccant system. Renewable Energy 1993;3(6/7):661–8.
[37] Luo YM, Shao SQ, Xu HB, Tian CQ. Dehumidification performance of [EMIM] BF_4. Appl Ther Eng 2011;31(14–15):2772–7.
[38] Luo YM, Shao SQ, Qin F, Tian CQ, Yang HX. Investigation of feasibility of ionic liquids used in solar liquid desiccant air conditioning system. Sol Energy 2012;86:2718–24.
[39] Liu XH, Jiang Y, Qu KY. Heat and mass transfer model of cross flow liquid desiccant air dehumidifier/regenerator. Energy Convers Manage 2007;48:546–54.
[40] Niu RP. Modeling and numerical simulation of dehumidifier using LiCl solution as the liquid desiccant. in: Proceedings of the international conference on electrical engineering and automatic control, Shandong; 2010.
[41] Woods J, Kozubal E. A desiccant-enhanced evaporative air conditioner: numerical model and experiments. Energy Convers Manage 2012;65:208–20.
[42] Stevens DI, Braun JE, Klein SA. An effectiveness model of liquid-desiccant system heat/mass exchangers. Sol Energy 1989;42(6):449–55.
[43] Braun JE. Methodologies for the design and control of chilled water systems [Ph.D. thesis in Mechanical Engineering], University of Wisconsin-Madison; 1988.
[44] Sadasivam M, Balakrishnan AR. Effectiveness-NTU method for design of packed bed liquid desiccant dehumidifiers. Chem Eng Res Des 1992;70:572–7.
[45] Jaber H, Webb RL. Design of cooling towers by the effectiveness-NTU method. J Heat Transfer 1989;111:837–43.
[46] Ren CQ. Corrections to the simple effectiveness-NTU method for counterflow cooling towers and packed bed liquid desiccant–air contact systems. Int J Heat Mass Transfer 2008;51:237–45.
[47] Liu XH, Qu KY, Jiang Y. Empirical correlations to predict the performance of the dehumidifier using liquid desiccant in heat and mass transfer. Renewable Energy 2006;31:1627–39.
[48] Gandhidasan P. A simplified model for air dehumidification with liquid desiccant. Sol Energy 2004;76:409–16.
[49] Gandhidasan P. Reconcentration of aqueous solutions in a packed bed: a simple approach. Trans ASME J Sol Energy Eng 1990;112:268–72.
[50] Kim KJ, Ameel TA, Wood BD. Performance evaluation of LiCl and LiBr for absorber design applications in the open-cycle absorption refrigeration system. Trans ASME J Sol Energy Eng 1997;119:165–73.

[51] Chen XY, Li Z, Jiang Y, Qu KY. Analytical solution of adiabatic heat and mass transfer process in packed-type liquid desiccant equipment and its application. Sol Energy 2006;80:1509–16.
[52] Ren CQ, Jiang Y, Zhang YP. Simplified analysis of coupled heat and mass transfer processes in packed bed liquid desiccant-air contact system. Sol Energy 2006;80(1):121–31.
[53] Babakhani D, Soleymani M. Simplified analysis of heat and mass transfer model in liquid desiccant regeneration process. J Taiwan Inst Chem Eng 2006;41:1509–16.
[54] Babakhani D, Soleymani M. An analytical solution for air dehumidification by liquid desiccant in a packed column. Int Commun Heat Mass Transfer 2009;36:969–77.
[55] Babakhani D. Developing an application analytical solution of adiabatic heat and mass transfer processes in a liquid desiccant dehumidifier/regenerator. Chem Eng Technol 2009;32(12):1875–84.
[56] Liu XH, Jiang Y, Qu KY. Analytical solution of combined heat and mass transfer performance in a cross-flow packed bed liquid desiccant air dehumidifier. Int J Heat Mass Transfer 2008;51:4563–72.
[57] Nusselt W. Der Warmeubergang im Kreuzstrom. Z Ver Dtsch Ing 1911;55: 2021–4.
[58] Nusselt W. Eine neue Formel fur den Warmedurchgang im Kreuzstrom. Tech Meahanik Thermodynamik 1930;1:417–22.
[59] Wang XL, Cai WJ, Lu JG, Sun YX, Ding XD. A hybrid dehumidifier model for real-time performance monitoring, control and optimization in liquid desiccant dehumidification system. Appl Energy 2013;111:449–55.
[60] Park JY, Jeong JWA. Simplified model for predicting dehumidification effectiveness of a liquid desiccant system. AEI 2013:516–23.
[61] Ren CQ, Tu M, Wang HH. An analytical model for heat and mass transfer processes in internally cooled or heated liquid desiccant-air contact units. Int J Heat Mass Transfer 2007;50:3545–55.
[62] Khan AY, Martinez JL. Modelling and parametric analysis of heat and mass transfer performance of a hybrid liquid desiccant absorber. Energy Convers Manage 1998;39(10):1095–112.
[63] Saman WY, Alizadeh S. Modelling and performance analysis of a cross-flow type plate heat exchanger for dehumidification/cooling. Sol Energy 2001;70 (4):361–72.
[64] Zhang T, Liu XH, Jiang JJ, Chang XM, Jiang Y. Experimental analysis of an internally-cooled liquid desiccant dehumidifier. Build Environ 2013;60:1–10.
[65] Qi RH, Lu L, Yang HX. Development of simplified prediction model for internally cooled/heated liquid desiccant dehumidification system. Energy Build 2013;59:133–42.
[66] Qi RH, Lu L, Yang HX. Quick performance prediction for internally cooled/heated liquid desiccant dehumidification system. Build Serv Eng Res Technol 2012, http://dx.doi.org/10.1177/0143624412468890.
[67] Ali A, Vafai K, Khaled ARA. Comparative study between parallel and counter flow configurations between air and falling film desiccant in the presence of nanoparticle suspensions. Int J Energy Res 2003;27:725–45.
[68] Ali A, Vafai K, Khaled ARA. Analysis of heat and mass transfer between air and falling film in a cross flow configuration. Int J Heat Mass Transfer 2004;47:743–55.
[69] Ali A, Vafai K. An investigation of heat and mass transfer between air and desiccant film in an inclined parallel and counter flow channels. Int J Heat Mass Transfer 2004;47:1745–60.
[70] Mesquita LCS, Harrison SJ, Thomey D. Modeling of heat and mass transfer in parallel plate liquid-desiccant dehumidifiers. Sol Energy 2006;80:1475–82.
[71] Dai YJ, Zhang HF. Numerical simulation and theoretical analysis of heat and mass transfer in a cross flow liquid desiccant air dehumidifier packed with honeycomb paper. Energy Convers Manage 2004;45:1343–56.
[72] Hueffed AK, Chamra LM, Mago PJ. A simplified model of heat and mass transfer between air and falling-film desiccant in a parallel-plate dehumidifier. J Heat Transfer 2009;131(5):052001-1–7.
[73] Peng SW, Pan ZM. Heat and mass transfer in liquid desiccant air-conditioning process at low flow conditions. Commun Nonlinear Sci Numer Simulation 2009;14:3599–607.
[74] Diaz G. Numerical investigation of transient heat and mass transfer in a parallel-flow liquid-desiccant absorber. Heat Mass Transfer 2010;46:1335–44.